VISIBLE/NIR SPECTROSCOPY FOR CHARACTERIZING FECAL CONTAMINATION OF CHICKEN CARCASSES

W. R. Windham, K. C. Lawrence, B. Park, R. J. Buhr

ABSTRACT. *Zero tolerance of feces on the surfaces of meat and poultry carcasses during slaughter was established as a standard to minimize the likelihood of microbial pathogens. Microbial pathogens can be transmitted to humans by consumption of contaminated meat and poultry. Compliance with zero tolerance of feces in meat processing establishments is currently verified by visual observation. The objective of this study was to investigate the use of visible, near–infrared reflectance spectroscopy as a method to discriminate between uncontaminated poultry breast skin and feces, and to select key wavelengths for use in a hyperpspectral system. Feces (n = 102), uncontaminated poultry breast skin, and skin contaminated with fecal spots were analyzed from 400 to 950 nm. The spectra were reduced by principal component (PC) analysis. The first four PCs explained 99.8% of the spectral variation. PC 1 was primarily responsible for the separation of uncontaminated skin from feces and for the separation of uncontaminated skin from contaminated skin. A classification model was developed and evaluated to classify fecal–contaminated skin from the spectral data with a success rate of 95%. Key wavelengths were identified by intensity of loading weights at 628 nm for PC 1, 565 nm for PC 2, and 434 and 517 nm for PC 4. Discrimination was dependent on the spectral variation related to fecal color and myoglobin and/or hemoglobin content of the uncontaminated breast skin.*

Keywords. *Contaminant, Feces, Poultry, Principal component analysis, Visible/NIR spectroscopy.*

Contamination of meat and poultry with bacterial food–borne pathogens can potentially occur because of exposure of the animal carcass to ingesta and/or fecal material during or after slaughter. Microbial pathogens can be transmitted to humans by consumption of contaminated undercooked or mishandled meat and poultry. Bacterial pathogens in food cause an estimated 76 million cases of human illnesses and up to 5,000 deaths annually (Mead et al., 1999).

Zero tolerance of feces on the surfaces of meat and poultry carcasses during slaughter was established as a standard by the Food Safety Inspection Service (FSIS) to minimize the likelihood of bacterial pathogens (USDA, 1994). In 1996, FSIS adopted the Pathogen Reduction, Hazard Analysis and Critical Control Points (HACCP) systems, requiring meat processing establishments to identify all food safety hazards in their process and to identify critical control points adequate to prevent them (USDA, 1996). Preventing carcasses with visible fecal contamination from entering the chlorinated ice water tank (chiller) is critical for preventing cross–contamination of other carcasses. Thus, the final carcass wash, before entering the chiller, has been adopted by many poultry processors as an HACCP system critical control point to remove all surface–adhering feces.

Compliance with zero tolerance in meat processing establishments is currently verified by visual observation. Three criteria are used for identifying fecal contamination: color, consistency, and composition. In general, fecal material color ranges from varying shades of yellow to green, brown, and white; the consistency of feces is usually semi–solid to paste; and the composition of feces may include plant material. Inspectors use these guidelines to verify that establishments prevent carcasses with visible fecal contamination from entering the chillers. Real–time visual inspection is both labor intensive and prone to both human error and variability.

Efforts have been made to develop automated or semi–automated visual inspection systems for detecting the presence of contaminants on food products during processing. These systems utilize a technique in which the food item is illuminated with UV or visible light, and emissions of fluorescent light are measured between 660 to 680 nm as an indication of the presence of fecal material (Waldroup and Kirby, 1997; Casey et al., 1999). Visible (Vis) and near–infrared reflectance (NIR) spectroscopy is a technique that can also be used to detect contamination on foodstuffs. The use of the Vis/NIR spectroscopic technique for classifying wholesome, septicemic, and cadaver carcasses has been reported by Chen and Massie (1993) and Chen et al. (1996). These studies were conducted with an NIR probe in contact with a stationary carcass. More recently, Chen and Hruschka (1998) reported an on–line transportable Vis/NIR system (400 to 1700 nm) in which the probe was not in contact with the carcass and carcasses were moving at rates of either 60 or 90 birds per minute. Carcasses were classified as wholesome

Article was submitted for review in October 2001; approved for publication by the Food & Process Engineering Institute Division of ASAE in February 2003. Presented at the 2001 ASAE Annual Meeting as Paper No. 016004.

The authors are **William R. Windham,ASAE Member,** Animal Scientist, **Kurt C. Lawrence,ASAE Member Engineer,** Agricultural Engineer, **Bosoon Park, ASAE Member Engineer,** Agricultural Engineer, and **Jeff Buhr,** Animal Scientist, USDA–ARS Richard B. Russell Research Center, Athens, Georgia. **Corresponding author:** W. R. Windham, USDA–ARS Richard B. Russell Research Center, P.O. Box 5677, Athens, GA 30604; phone: 706–546–3513; fax: 706–546–3633; e–mail: rwindham@saa.ars.usda.gov.

or unwholesome with an average accuracy of 94% and 97.5% when measured in room light and in the dark, respectively. The Vis/NIR method showed promise for separation of wholesome and unwholesome carcasses in a partially automated system.

Multispectral and hyperspectral imaging systems also have the potential for inspection of foods during food processing. Multispectral imaging consists of measurements from two to about ten discrete wavelengths for a given image; hyperspectral imaging measures more than ten contiguous wavelengths. Like multispectral imaging, hyperspectral imaging is a technique that combines aspects of conventional imaging with spectrometry and radiometry. The result is a technique that is capable of providing an absolute radiometric measurement over a contiguous spectral range for each pixel of an image. Thus, data from a hyperspectral image contains two–dimensional spatial information plus spectral information over the spatial image. Since biological materials at different conditions have different spectral reflectance characteristics, the status of materials could be identified based on their spectral images by selecting optimum wavelengths.

Hyperspectral imaging has been used for the identification of surface contaminates on poultry carcasses (Lu and Chen, 1998; Heitschmidt et al., 1998). Hyperspectral and multispectral imaging techniques were used to detect chicken skin tumors (Chao et al., 2000). Park et al. (2001) reported a hyperpspectral imaging system for detecting feces and ingesta on the surfaces of poultry carcasses. However, many of the spectra from the hyperspectral system were not analyzed to determine the optimal wavelengths needed for fecal identification. Therefore, the objectives of this research are to investigate the use of Vis/NIR spectroscopy to discriminate between uncontaminated poultry breast skin and feces and to select key wavelengths for use in a multispectral or hyperpspectral system.

Materials and Methods

Broilers and Housing

Male broilers were obtained from a local commercial farm (38 days old) and transported to grow–out facilities. The broilers were transported for less than 30 min and were placed 20 per pen into 2.4 × 3 m floor pens covered with wood shavings. Broilers were provided a non–medicated, corn–soybean meal pelleted growers diet (3,200 kcal ME/kg, 19% crude protein) ad libitum. The evening before processing, feed was removed for 4 h. Feed was then offered to ensure a consistent amount of fecal material in the digestive tract among broilers. After 2 h of meal feeding, feed was removed for 4 h, but water remained available for 4 h prior to catching. At catching, 10 broilers were put into coops (two coops per pen), and held for 4 h prior to processing.

Processing Procedures

Broilers were stunned head to shanks while moving through an in–line brine stunner (Simmons) and bled with a Simmons SK–5 automated knife. Broilers were bled in shackles for a total of 120 s, scalded at 56.7°C for 120 s in a scalder containing approximately 2,000 L water, and then defeathered with a single–pass picker (Johnson Food Equipment Co., Kansas City, Kansas) for 30 s. After defeathering, heads were removed with hand shears (between the second and fourth cervical vertebrae). To collect intestinal contents, the abdominal cavity was opened transversely to allow sufficient manual evisceration. The duodenum, ceca, and colon were each clamped at the proximate and distal ends with two 6–inch hemostatic forceps and sectioned with hand scissors. When fecal contents were available, feces was pressed from the excised segments into sample vials for analysis by visible/NIR spectroscopy. When possible, three circular skin samples were taken from the breast area of the carcass and placed in plastic bags for analysis by visible/NIR spectroscopy. This experiment was replicated two times with twenty 6–week–old broilers obtained from different farms.

Spectroscopic Signal Acquisition

Duodenum, ceca, and colon feces, breast skin, and breast skin contaminated with feces were scanned with an NIRSystems 6500 monochromator (NIRSystems, Silver Spring, Md.) having a tungsten source and a holographically ruled grating. Spectra were recorded from 400 nm to 2500 nm in 2–nm intervals. The lower wavelength region (400 to 1098 nm) was acquired by a pair of silicon detectors located 20 cm from the surface of the sample cell and at an angle of 45° to the incident beam. The upper wavelength region (1100 to 2498 nm) was acquired by a pair of lead sulfide detectors in the same orientation as the silicon detectors. Reference reflectance values were obtained using a ceramic block. Samples of feces were presented in cylindrical sample cells (38 mm I.D.; 0.1, 0.2, or 0.3 mm depth) with optical quartz surfaces and locking backs. Three circular replicates of uncontaminated breast skin from each carcass were presented in cylindrical sample cells (38 mm I.D., 9 mm depth) with optical quartz surfaces and cardboard backing. After scanning, the sample cell with the first skin replicate was opened and contaminated with about a 3 to 6 mm diameter spot of duodenum feces. Similarly, replicates 2 and 3 were contaminated with ceca and colon feces, respectively. Each sample was scanned 32 times, averaged, and transformed to log(1/reflectance).

Multivariate Analysis

A commercial spectral analysis program (NIRS3, Infrasoft International, Inc., Port Matilda, Pa.) was used to analyze the spectral data. Principal component analysis (PCA) (Marten and Naes, 1989, pp. 237–266) was used to evaluate uncontaminated skin and feces. Partial least squares regression (PLSR) (Marten and Naes, 1989, pp. 237–266) was used to evaluate uncontaminated skin and skin contaminated with fecal spots. Spectra were analyzed from 400 nm to 950 nm to correspond to the wavelength range of the hyperspectral imaging system described by Park et al. (2001). Based on the experimental design, the number of uncontaminated skin samples and each fecal type was 120 and 40, respectively. However, not all samples were available for analysis. The breast surface area of some carcasses was not large enough to obtain three circular replicates of uncontaminated breast skin. In addition, the excised ceca and colon segments from 3 and 15 carcasses, respectively, did not contain enough fecal material to complete fill the cylindrical sample cell for the PCA dataset. In the PLSR dataset, there was enough ceca and colon material obtained from three of these carcasses to contaminated the skin with a 3 to 6 mm diameter spot.

The PCA spectral dataset (n = 102 uncontaminated skin, n = 40 duodenum, n = 37 ceca, and n = 25 colon) was transformed with multiplicative scatter correction (MSC) (Isaksson and Naes, 1988). Spectra were mean centered and reduced by PCA (Cowe and McNicol, 1985). The PLSR spectral dataset (n = 108 uncontaminated skin, contaminated with n = 40 duodenum, n = 40 contaminated with ceca, and n = 28 contaminated with colon) was also transformed with MSC. PLSR was used to relate the mean–centered spectra to the dummy variable 1 for uncontaminated skin and 2 for contaminated skin. To perform PLSR, we needed a decision on the number of factors needed to obtain a good prediction. For this purpose, we used full cross–validation (Martens and Naes, 1989, pp. 237–266). One spectrum was removed from the data matrix, the corresponding reference value (i.e., 1 for uncontaminated skin and 2 for contaminated skin) was removed from the reference value matrix, and a model was built on the remaining samples. The model was then used to estimate value for the sample that was left out. This process was repeated until each sample had been left out. Performance statistics were accumulated for each sample removed. The optimal number of PLSR factors for the model was that which produced the first minimum in error between modeled and reference value for the samples removed during cross–validation.

Results and Discussion

Uncontaminated Breast Skin versus Feces

Figure 1 shows the average log(1/reflectance) spectra of uncontaminated breast skin and duodenum, ceca, and colon feces. In general, the feces spectra had greater absorbance than uncontaminated skin samples. The main difference was observed in the visible region (400 to 700 nm). This region represents the colors of the undigested plant pigments in the feces and the muscle pigment myoglobin in skin. Some hemoglobin may also be present in residual blood of the skin and could have an effect on the spectral characteristics.

The color of meat is largely determined by the relative amount of three forms of myoglobin, i.e., deoxymyoglobin, oxymyoglobin, and metmyoglobin (Price and Schweigert, 1987, pp. 155–343), at the meat surface. Liu and Chen (2000) reported at least seven absorption bands at 430, 440, 455, 545, 560, 575, and 585 nm associated with the changes in the oxidation and denaturation of myoglobin due to cooking and cold storage. Uncontaminated skin had absorption bands at 424, 544, and 570 nm (fig. 1). The bands at 544 and 570 nm are attributed to oxymyoglobin, and the band at 424 nm can be assigned to the Soret absorbance band for oxymyoglobin (Swatland, 1989)

The feces spectra represent a mixture of plant pigments with broad absorbance, which increase with decreasing wavelength. Fecal material obtained from the three different segments varied greatly in color. In general, colon and cecal feces were brown to dark brown in color compared to duodenum feces, which was yellow–orange to light brown. Feces spectra decreased in absorbance at 458 nm as fecal material became browner. The cecal and colon feces had a greater broad absorbance characteristic (525 to 725 nm) than duodenum feces.

Prior to PCA, the spectral dataset was transformed with MSC to remove interferences of light scatter from the skin and differences in pathlength due to feces sample thickness variations. PCA is a projection method for extraction of the systematic variations in a dataset resulting in principal component models. Translated into principal components (PC), the new coordinate system has fewer dimensions than the original Vis/NIR dataset, and the directions of the new coordinate axes (called principal components) were calculated to describe the largest variations. The localizations of the samples in the new system (i.e., their coordinates related to the PCs) are called scores. Scores calculated from these components were plotted as shown in figure 2.

The first four components accounted for 98% of the total spectral variation, with components 1, 2, and 4 expressing 92% of the variation. Scores from the first PC separated the uncontaminated skin from contaminants regardless of fecal type. Uncontaminated skin had negative scores, whereas feces had positive scores. PC 2 and 4 separated fecal type. Fecal type was distributed along the axes of the second PC, indicating its wide variation. In addition, there was less spectral variation in feces from the duodenum compared to ceca and colon feces. In an overall evaluation, the first PC is clearly related to the uncontaminated skin, while the second and fourth PCs describe the variations of fecal type. These results demonstrate the ability to discriminate between uncontaminated skin and feces due to the variations in the

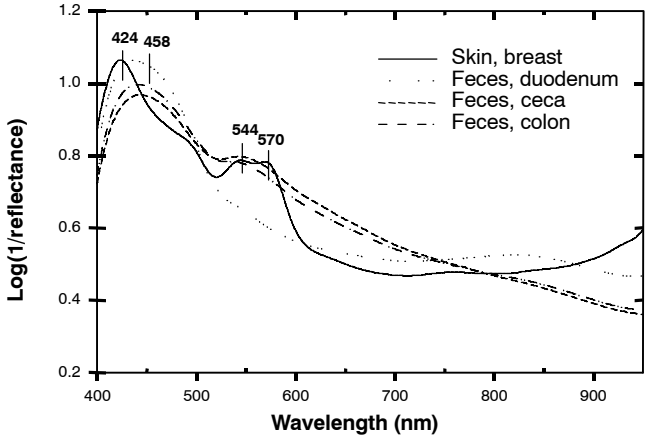

Figure 1. Average absorbance [log(1/reflectance)] spectra of uncontaminated breast skin and feces from duodenum, ceca, and colon.

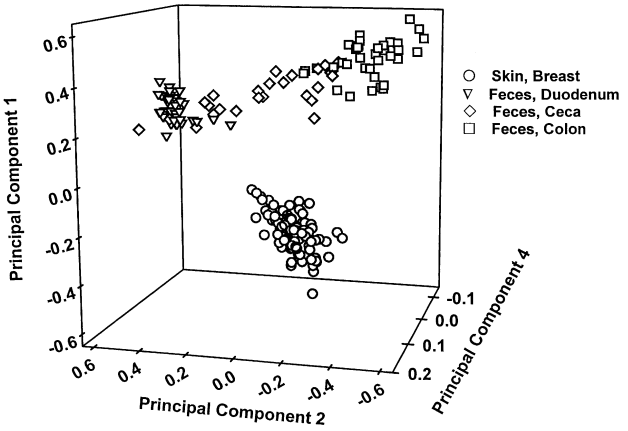

Figure 2. PCA score plot of components 1, 2, and 4 for uncontaminated breast skin and duodenum, ceca, and colon feces.

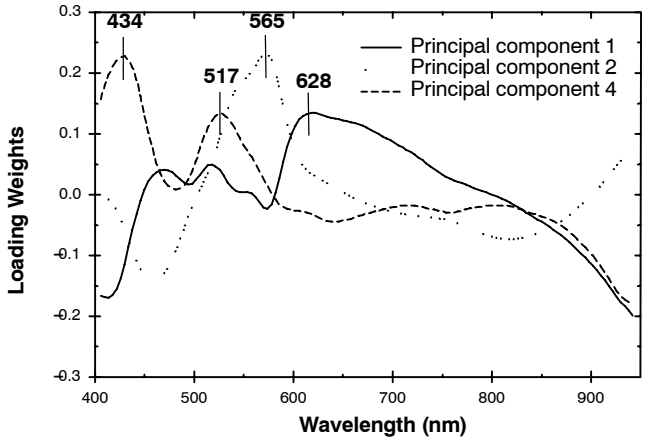

Figure 3. Loading weights of principal components 1, 2, and 4 for uncontaminated breast skin and feces.

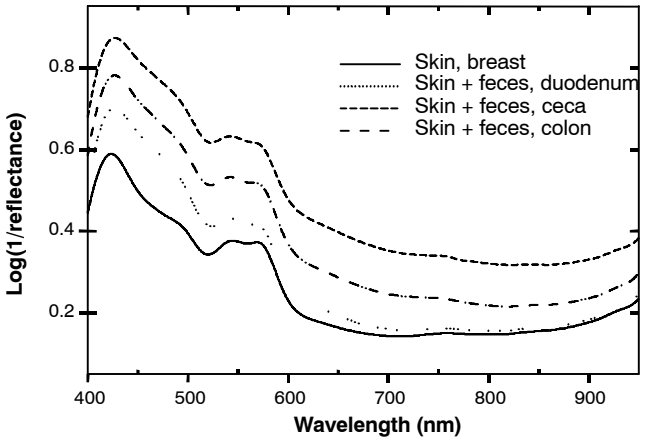

Figure 4. Average absorbance [log(1/reflectance)] spectra of uncontaminated breast skin and skin contaminated with duodenum, ceca, and color feces.

Vis/NIR spectra, which arise from the intrinsic differences in color and chemical constituents of the samples.

Loadings are the regression coefficients of each variable (wavelength) for each PC. Loadings often resemble the spectra of samples and the spectra of constituents and thus offer scope for interpretation of maximum weighting matching known absorbance bands (Cowe and McNicol, 1985). The loadings of the PCs, used to discriminate between uncontaminated breast skin and feces, are shown in figure 3. The loading plot indicates how the variance is accounted for in a PC across the wavelength scale. Numerically higher (+/–) weights indicate a relative high contribution of the wavelength area to that PC.

The shape of the plot for the first PC showed the broad absorbance (628 nm) characteristic of feces color compared to the color of uncontaminated skin. Uncontaminated skin had lower absorbance (fig. 1) than feces in this wavelength region. Weights 2 and 4 had large intensities at 565 and 434 nm, respectively, related to the myoglobin and/or hemoglobin of the breast skin. Weight 4 also had significant intensity at 517 nm, possibly related to color differences.

Uncontaminated Breast Skin versus Fecal-Contaminated Breast Skin

Breast skin was contaminated with feces varying in spot size from about 3 to 6 mm. However, the spot size of contamination increased when the cardboard backing was pressed into the sample cell. Ceca samples had a paste consistency resulting in a fairly uniform or contiguous spot, whereas duodenum and colon samples had a liquid consistency resulting in a dispersed spot on average. Duodenum, colon, and ceca spots covered 10.0% ±4.5%, 10.2% ±4.4%, and 10.2% ±3.1%, respectively, of the skin surface area. Contaminated skin spectra not transformed with MSC retained the overall absorbance features of uncontaminated skin (fig. 4). However, contaminated skin had a greater overall absorbance than uncontaminated skin. The spectral absorbance of contaminated skin varied due to fecal type. Skin contaminated with ceca feces had a greater absorbance than skin contaminated with duodenum or colon feces. These results are in agreement with the absorbance of feces (fig. 1).

Spectra of uncontaminated and contaminated skin were transformed with MSC and correlated with the dummy variable 1 for uncontaminated and 2 for contaminated skin. Spectra of skin contaminated with fecal spots decreased in absorbance at 458 nm as the spots became browner (fig. 5). Contaminated samples had a broad absorbance (525 to 700 nm), which increased as the contaminated became darker. The absorbance characteristics of the contaminated skin were in agreement with the spectra of feces (fig. 1). The resulting correlation plot (fig. 5) shows the best correlation at the broad absorbance (600 to 730 nm), in agreement with the wavelength region for absorption of fecal color. The next best correlation is at 400 to 435 nm, which is related to myoglobin. However, this wavelength region cannot be used in the hyperspectral imaging system due to low signal–to–noise ratio. A good correlation also occurs at 458 and 517 nm, which is related to fecal color. Absorption of oxymyoglobin at 544 and 570 nm were negatively correlated.

A PLSR calibration was obtained for classification of fecal spots on skin (contaminated skin). The multiple coefficient of determination, with full cross–validation, was 0.79. The model correctly classified 94.5% of the contaminated samples correctly. The equation contained eight components, with scores from components 1, 4, and 5 having correlations of 0.60, 0.07, and 0.05, respectively, with the dummy variable 1 for uncontaminated skin and 2 for contaminated skin. The eight components explained 83% of the spectral variation. Sample scores calculated from these components were plotted as shown in figure 6. Scores from

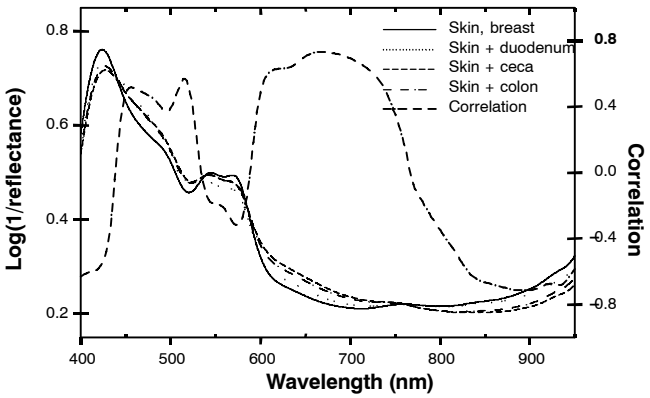

Figure 5. Average multiplicative scatter–corrected spectra of uncontaminated skin and skin contaminated with duodenum, ceca, and colon feces and correlation spectrum.

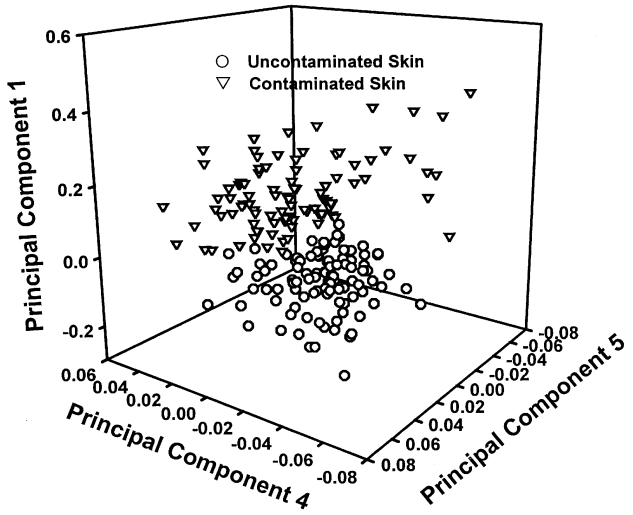

Figure 6. PLS score plot of components 1, 4, and 5 for uncontaminated skin and skin contaminated with fecal spots.

the first component separated uncontaminated skin from skin contaminated with fecal spots. Uncontaminated skin had negative scores, whereas samples with fecal spots had positive scores. This separation is in agreement with PCA of uncontaminated skin and feces (fig. 2). However, scores from PLSR regression could not separate fecal type. PLSR loadings were similar in shape and weight intensity to PCA.

Summary and Conclusions

Visible/near–infrared spectroscopy from 400 to 950 nm was used to discriminate between uncontaminated poultry breast skin and fecal material from different segments of the digestive tract. A PLSR classification model was able to classify fecal–contaminated skin from log(1/reflectance) spectral data with a success rate of 94.5%. Assessment of PCA and PLSR loadings suggested that discrimination was dependent on the spectral variation related to fecal color and myoglobin of the uncontaminated breast skin. The key wavelengths were identified by intensity of principal component loadings. Wavelengths selected were 628 nm for principal component 1, 565 nm for principal component 2, and 434 and 517 nm for principal component 4.

References

Casey, T. A., M. A. Rasmussen, and J. W. Petrich. 1999. Method and system for detecting fecal and ingesta contamination on the carcasses of meat animals. U.S. Patent No. 5,914, 247.

Chen, Y. R., and D. R. Massie. 1993. Visible/near–infrared reflectance and interactance spectroscopy for detection of abnormal poultry carcasses. *Trans. ASAE* 36(3): 863–889.

Chen, Y. R., and W. R. Hruschka. 1998. On–line trials of a chicken carcass inspection system using visible/near–infrared reflectance. ASAE Paper No. 983047. St. Joseph, Mich.: ASAE.

Chen, Y. R., R. W. Huffman, B. Park, and M. Nguyen 1996. Transportable spectrophotometer system for on–line classification of poultry carcasses. *Applied Spectroscopy* 50(7): 910–916.

Chao, K., P. M. Mehl, and Y. R Chen. 2000. Use of hyper– and multi–spectral imaging for detection of chicken skin tumors. ASAE Paper No. 003084. St. Joseph, Mich.: ASAE.

Cowe, I. A., and J. W. McNicol. 1985. The use of principal components in the analysis of near–infrared spectra. *Applied Spectroscopy* 39(2): 257–266.

Heitschmidt, J., M. Lanoue, C. Mao, and G. May. 1998. Hyperspectral analysis of fecal contamination: A case study of poultry. *Proc. SPIE* 3544: 134–137.

Isaksson, T., and T. Naes. 1988. The effect of multiplicative scatter correction (MSC) and linearity improvement in NIR spectroscopy. *Applied Spectroscopy* 42(7): 1273–1284.

Liu, Y., and Y. R. Chen. 2000. Two–dimensional correlation spectroscopy study of visible and near–infrared spectral variation of chicken meats in cold storage. *Applied Spectroscopy* 54(10): 1458–1470.

Lu, R., and Y. R. Chen. 1998. Hyperspectral imaging for safety inspection of food and agricultural products. *Proc. SPIE* 3544: 121–133.

Martens, H., and T. Naes. 1989. *Multivariate Calibration*. New York, N.Y.: Wiley.

Mead, P. S., L. Slutsker, V. Dietz, L. F. McCaig, J. S. Bresee, C. Shapiro, P. M. Griffin, and R. V. Tauxe. 1999. Food–related illness and death in the United States. *Emerging Infectious Diseases* 5(6): 607–625.

Park, B., K. C. Lawrence, W. R. Windham, and R. J. Buhr. 2001. Hyperspectral imaging for detecting fecal and ingesta contamination on poultry carcasses. ASAE Paper No. 013130. St. Joseph, Mich.: ASAE.

Price, J., and B. Schweigert. 1987. *The Science of Meat and Meat Products.* 3rd ed. Westport, Conn.: Food and Nutrition Press.

Swatland, H. J. 1989. A review of meat spectrophotometry (300 to 800 nm). *Canadian Inst. Food Science and Tech. J.* 22: 390–402.

USDA. 1994. Enhanced poultry inspection. Proposed rule. Federal Register 59:35659.

_____. 1996. Pathogen reduction, hazard analysis, and critical control point (HACCP) systems. Final Rule. Federal Register 61:28805–38855.

Waldroup, A., and J. Kirby. 1997. Method and system for fecal detection. U.S. Patent No. 5, 621, 215.